



**HAL**  
open science

## Exploring the inhibition of targeted microalgae by a *Cylindrotheca closterium* non-axenic biofilm

Lucie Sanchez, Amandine Avouac, Emilie Le Floc'H, Christine Félix,  
Christophe Leboulanger, Angélique Gobet, Eric Fouilland

### ► To cite this version:

Lucie Sanchez, Amandine Avouac, Emilie Le Floc'H, Christine Félix, Christophe Leboulanger, et al..  
Exploring the inhibition of targeted microalgae by a *Cylindrotheca closterium* non-axenic biofilm.  
Journal of Applied Phycology, In press. hal-04662985v2

**HAL Id: hal-04662985**

**<https://hal.science/hal-04662985v2>**

Submitted on 13 Dec 2024

**HAL** is a multi-disciplinary open access archive for the deposit and dissemination of scientific research documents, whether they are published or not. The documents may come from teaching and research institutions in France or abroad, or from public or private research centers.

L'archive ouverte pluridisciplinaire **HAL**, est destinée au dépôt et à la diffusion de documents scientifiques de niveau recherche, publiés ou non, émanant des établissements d'enseignement et de recherche français ou étrangers, des laboratoires publics ou privés.

1 **Exploring the inhibition of targeted microalgae by a *Cylindrotheca closterium* non-axenic**  
2 **biofilm**

3

4 Lucie Sanchez, Amandine Avouac, Emilie le Floc'h, Christine Félix, Christophe Leboulanger,  
5 Angélique Gobet and Eric Fouilland\*

6

7 MARBEC, Univ Montpellier, CNRS, Ifremer, IRD, Sète, France

8 \*corresponding author: eric.fouilland@cnrs.fr

9

10 **Abstract.** While most studies on allelopathic interactions among autotrophic microorganisms  
11 focus on free-living aquatic species, little is known about microalgal biofilms, where chemical  
12 communication is enhanced by spatial proximity. A co-culture protocol using a disc diffusion  
13 method was developed to assess the inhibitory potential of the marine diatom *Cylindrotheca*  
14 *closterium* growing in non-axenic conditions, against different targeted algal strains. The  
15 biofilm exhibited an inhibitory effect on the individual growth of two algal strains,  
16 *Nannochloropsis oculata* and *Tetraselmis striata*, but did not affect the microalga  
17 *Porphyridium purpureum*. The findings highlight the potential of such allelopathic interactions,  
18 making *C. closterium* a candidate for contamination-resistant algal biofilm technologies.  
19 Further research is needed to identify the inhibitory compounds and their microbial producers  
20 within the growing biofilm.

21

22

23 **Keywords** Microalgae, Allelopathic interactions, Biofilm, Bacteria, Microbial co-culture

24

25

26 **Introduction**

27

28 The dominance of algal species in a nutrient-rich environment may be explained by exclusive  
29 resource competition or grazing selectivity (Vallina et al. 2014). However, interactions within  
30 algal communities may also occur by allelopathy (Legrand et al. 2003), defined as a chemical  
31 communication involved in inter-species competition, where one species prevents other  
32 organisms from using available resources by producing effective molecules. Distinguishing  
33 competition from allelopathy under natural conditions remains difficult (Inderjit and del Moral  
34 1997). If competition is mainly characterized by the species intrinsic ability for resource

35 acquirement, the allelopathic effects depend on the sensitivity and physiological status of the  
36 targeted organism, the distance between the emitter and the target, and the concentration of  
37 produced molecules (Leflaive and Ten-Hage 2007). Therefore, allelopathic interactions are  
38 particularly expected in aquatic biofilms because organisms are physically close (Allen et al.  
39 2016). When lipophilic, allelochemical compounds can readily diffuse through extracellular  
40 polymeric substances constituting biofilm matrix, or direct cell-to-cell contact, reducing their  
41 dilution. Their concentration can therefore be significant in the biofilm while being less  
42 detectable in the surrounding water (Allen et al. 2016, Uchida 2001). Allelopathic compounds  
43 may be produced to target planktonic organisms. In this case, these molecules must be  
44 sufficiently concentrated to affect targets over greater distances in a diluted aquatic  
45 environment (Gross 2003).

46         Diatoms are species known for the production of inhibitory compounds, such as  
47 polyunsaturated fatty acids (PUFAs), polyunsaturated aldehydes (PUAs), polyphenolic and  
48 halogenated compounds that have been proven to negatively impact other microalgae (Pichi  
49 et al. 2017; Wenjing et al. 2019). The marine diatom *Cylindrotheca closterium*, living both as  
50 free-floating cells or in biofilm, displays allelopathy abilities when cultured in planktonic form  
51 (Wenjing et al. 2019). However, the allelopathy ability of *C. closterium* when growing in  
52 biofilm is unknown. A phototrophic biofilm is a microbial cell association (including  
53 autotrophic and heterotrophic microbes) that secretes insoluble exopolysaccharides, which  
54 enable the formation of a matrix at the interface between the water column and solid surfaces  
55 in aquatic environments (Donlan, 2002). In phototrophic biofilms, primary production and  
56 remineralization processes occur simultaneously. The high microbial cell density usually found  
57 in biofilms is suggested to protect them against dilute inhibitory or toxic compounds (Allen et  
58 al 2016). Still, the demonstration of autotrophic biofilms acting as a potential allelochemical  
59 emitter or as an inhibition-resistant community has not been clearly shown due to lack of  
60 suitable method (Allen et al 2016). Numerous studies utilize biomass extracts from benthic  
61 microalgae for testing allelopathy bioassays. However, biomass extracts may contain  
62 compounds that are never released by the living cells, making it challenging to demonstrate the  
63 excretion of allelochemicals when they do not diffuse into the surrounding medium.  
64 Furthermore, most studies investigating allelopathy between algae used non-axenic cultures  
65 without considering the ability of bacteria to produce inhibitory or algicidal compounds in the  
66 biofilm (Coyne et al. 2022). In addition, they usually used filtered dissolved fractions from  
67 algal growth medium although some of the allelopathic compounds required to be continuously  
68 produced to be effective (Flores et al. 2012). More suitable methods are therefore requested to

69 consider the co-existence of various species of algae as well as bacteria in the biofilm and test  
70 their role as potential emitter and/or target. Previous studies have used classical agar diffusion  
71 assays (Flores and Wolk 1986) to report inhibitory effects of cyanobacteria or fungi in biofilms  
72 on various bacteria or microalgae species (Allen et al. 2016). However, to the best of our  
73 knowledge, no studies have investigated co-culturing experiments involving algal biofilms as  
74 emitter and target.

75

76 The inhibitory activity of algal biofilms against potential competitors may be a valuable  
77 trait when cultivating commercially relevant algal species. Attached culture systems, an  
78 emerging technology replacing suspended culture systems, facilitate biomass growth as a  
79 biofilm on a support continually rotating between liquid and gaseous phases (Morales et al.  
80 2020). Recent works have highlighted the reduction of environmental impact of such new  
81 production systems (Morales et al. 2020, Penaranda et al. 2023). The long-term growth of  
82 microalgae in attached culture systems showing very little algal contamination during growing  
83 periods (F. Guiheneuf, personal communication), suggests potential allelopathy ability.

84

85 We therefore hypothesized that microalgae and associated bacteria established in  
86 biofilm under favorable growth conditions may have the ability to inhibit potential competitors  
87 such as allochthonous microalgae. To test this hypothesis, we examined the inhibitory potential  
88 of the diatom *Cylindrotheca closterium* when cultivated using a biofilm culture system under  
89 laboratory conditions. Inhibition tests were performed using experimental *C. closterium* biofilm  
90 co-cultures from a modified version of the disc diffusion method (Hudzicki 2009) against three  
91 selected microalgae targets. Two of the studied targets are pelagic marine microalgae,  
92 *Tetraselmis striata* and *Nannochloropsis oculata*, and belong to the Chlorophyta and  
93 Stramenopiles phyla, respectively. The third studied target was a marine benthic microalga,  
94 *Porphyridium purpureum*, belonging to the Rhodophyceae phylum. These microalgae were  
95 selected for inhibition tests because they can grow as a biofilm, and they belong to genera that  
96 are susceptible to inhibition (*Tetraselmis* and *Nannochloropsis*, Khairy 2010, Chaïb et al. 2021)  
97 or less sensitive to allelochemicals (*Porphyridium purpureum*, Hellio et al. 2002). In addition,  
98 those strains belong to different taxonomic clades, representing a broad representation of  
99 biological diversity, as well as a diversity in size, morphology, and pigments.

100

101

102

103 **Materials and methods**

104

105

106 **Selected microalgae strains**

107

108 The benthic diatom *Cylindrotheca closterium* AC170 was obtained from the Algalbank Caen  
109 Collection (Université de Caen Basse-Normandie, France) and used as a potential emitter. The  
110 selected target strains were: i) the planktonic Chlorophyta *Tetraselmis striata* isolated and  
111 identified in 2018 from a high-rate algal pond located in Palavas-les-flots (Southern France,  
112 Pascon et al. 2021), ii) the planktonic Stramenopiles *Nannochloropsis oculata* (CCAP 847/9)  
113 and iii) the benthic Rhodophyceae *Porphyridium purpureum* (CCAP 1380).

114

115 **Culture conditions**

116

117 Before experimentations, the four algal strains were cultured in planktonic mode using a  
118 modified f/2 medium by doubling concentrations of nitrate, phosphate and silicate (Guillard  
119 and Ryther 1962, Guillard 1975, Supl. Table 1), prepared with an artificial seawater basis  
120 (Instant Ocean, (Aquarium Systems) adjusted to achieve a salinity of 40. All cultures were  
121 incubated at 20 °C under continuous white light with a light intensity of 85  $\mu\text{mol photons m}^{-2}\cdot\text{s}^{-1}$ .

122 *Cylindrotheca closterium* was cultivated as a biofilm using a small rotating  
123 experimental culture system (Fig. 1) under controlled laboratory conditions (controlled  
124 temperature of 20 °C and light of 80-90  $\mu\text{mol photons}\cdot\text{m}^{-2}\cdot\text{s}^{-1}$ ) with weekly sterile culture  
125 medium addition. A plastic tank (L35 cm x W25 cm x H15 cm) was used and contained a roller  
126 with a length of 30 cm and a diameter of 10 cm, with a rotating bar allowing for tangential  
127 velocity ranging from 0.02 to 0.07  $\text{m}\cdot\text{s}^{-1}$ . A textile fabric was autoclaved and placed on the  
128 roller using zip ties. On March 10<sup>th</sup> 2023, the fabric was moistened on the roller with a sterile  
129 culture medium for one day and inoculated by evenly pouring onto the fabric the planktonic  
130 culture of *C. closterium* at 5.7 rotations per minute (rpm) under a light intensity of 90  $\mu\text{mol}$   
131  $\text{photons m}^{-2}\cdot\text{s}^{-1}$ . The plastic tank was then half-filled with 3.6 L of sterile culture medium,  
132 ensuring that  $\frac{3}{4}$  of the roller was exposed to the air while  $\frac{1}{4}$  was immersed in the culture  
133 medium. After 10 days and visual check of signs of biofilm establishment, the rotation speed  
134 was increased to 15 rpm and the light intensity was raised to 100  $\mu\text{mol photons m}^{-2}\cdot\text{s}^{-1}$  in order  
135 to ensure higher access to light and nutrients without risking biofilm detachment. Once the  
136

137 biofilm onto the fabric reached maturity after three weeks (characterized by a dark brown  
138 colour, uniformity, and opacity, see Fig. 1A), it was collected by scraping the entire fabric.  
139 After the first harvest from the fabric, the rotation speed was increased to 37 rpm, equivalent  
140 to a linear speed of 0.2 m s<sup>-1</sup> that is the optimal speed before inducing cell detachment (F.  
141 Guiheneuf, personal communication). The entire biofilm was harvested every three weeks. The  
142 biofilm that developed at the bottom of the tank was harvested every week before fresh culture  
143 medium renewal (Figure 1A). The harvested one-week biofilm at the bottom of the tank after  
144 14 days of experiment (March 24 2023, hereafter referred to as 14T) and after 131 days of  
145 experiment (July, 19 2023, 131T) and the harvested three-week biofilm from the fabric on the  
146 roller after 131 days of experiment (131R) were tested for potential inhibition on targeted  
147 microalgae strains.

148

#### 149 **Inhibition tests using *Cylindrotheca closterium* biofilm on targeted microalgae**

150 Inhibition tests were developed based on the paper disc antibiotic sensitivity testing design, to  
151 visualize the formation of an inhibition halo against an algal target spread on a Petri dish, from  
152 a disc on which *C. closterium* biofilm fraction was deposited (Fig. 2). To get homogeneous  
153 targeted algal mats, and for each of the targeted microalga, a sterile cotton swab with 6 mm  
154 cotton wool tip was dipped into the planktonic target microalgae culture in the exponential  
155 growth phase and streaked onto 1.5% agar-containing modified f/2 medium. For each targeted  
156 species, one such Petri dish was used as a control and three others for the inhibition tests. Once  
157 the targeted algal strain achieved uniform growth on the Petri dish (after about 14 days at 20  
158 °C under continuous white light at an intensity of 85 μmol photons.m<sup>-2</sup>.s<sup>-1</sup>), sterile cellulosic  
159 discs were carefully placed on the agar surface (Fig. 2). One disc was inoculated with 20 μL of  
160 positive control (35% hydrogen peroxide), another disc with 20 μL of negative control (sterile  
161 modified f/2 medium), a third disc was inoculated with the *C. closterium* biofilm and two other  
162 discs were inoculated after centrifuging the *C. closterium* biofilm at 4500 g for 10 minutes at  
163 20 °C. A volume of 20 μL was deposited on each disc with the respective pellet and raw  
164 supernatant of *C. closterium*. Centrifugation intended to separate the particulate from the  
165 dissolved fractions of the biofilm. Filtration at 0.2 μm using polycarbonate filter was also  
166 performed from *C. closterium* biofilm on roller fabric. The one-week biofilm of *C. closterium*  
167 that was developing at the bottom of the tank was sampled after 14 days and after 131 days of  
168 experiment, while the three-week *C. closterium* biofilm formed on the roller fabric was scraped  
169 after 131 days. After placing the two controls and biofilms onto the cellulosic discs, the Petri  
170 dishes were all incubated in duplicates for 14 days at 20 °C under continuous white light at an

171 intensity of 85  $\mu\text{mol photons}\cdot\text{m}^{-2}\cdot\text{s}^{-1}$ . After 14 days of incubation, the diameters of the inhibition  
172 zones when present were measured and observed under the inverted microscope to evaluate the  
173 presence, the shape and the size of the algal cells in these areas (Fig. 2).

174

#### 175 **Microscopical examination, cell size and shape evaluation**

176 Biofilm samples were examined using an Olympus ix53 inverted microscope equipped with a  
177 Kern ODC 832 CMOS camera. Image scaling was calibrated using an Optika M-005  
178 micrometric slide to determine pixel-to-micrometer ratios for each magnification using  
179 ToupTek Lite software. Depending on the species, the diameter (spherical cells), length and  
180 width (pennate diatoms) were measured for 20 individuals. Statistical analyses were conducted  
181 using a Mann-Whitney test to compare means from cell dimension measurements, with a  
182 significance level set at a  $p$ -value of 0.05.

183

#### 184 **Bacteria isolates from inhibition zones**

185 The potential role of bacteria in the inhibition activity was investigated. When inhibition zones  
186 around cellulosic discs were observed, samples were taken with an oese to isolate and identify  
187 the bacterial strains from these zones and to perform additional inhibition tests on targeted  
188 microalgae. Bacteria were isolated using serial dilutions (1/10, 1/100 and 1/1000), and then  
189 spread on Zobell agar medium to isolate colonies. The Petri dishes were incubated for eight  
190 days at 20 °C in the dark. Dilutions (1/10 or 1/100) that allowed the maximum number of  
191 identifiable bacterial colonies were preserved. Morphologically distinct colonies were isolated  
192 on new duplicated plates and incubated at 20°C in the dark until obtaining distinct and separate  
193 colonies (between 48 hours and 120 hours, depending on the bacterial strain). Individual  
194 colonies were then sub-cultured onto a new plate and incubated under the same conditions at  
195 least two more times to ensure strain purity.

196 The identification of isolated bacterial strains was carried out using a Sanger sequencing  
197 approach. A heat shock was performed on the bacterial cultures frozen at -20 °C, to a  
198 temperature of 95 °C for 15 minutes to access their DNA. Amplification of the 16S rRNA gene  
199 of each bacterial colony was then performed using universal primers: forward 8F (5'-  
200 AGAGTTTGATCCTGGCTCAG-3'; Edwards *et al.* 1989) and reverse 1492R (5'-  
201 CGGTTACCTTGTTACGACTT-3'; Stackebrandt and Liesack, 1993). A reaction mixture was  
202 prepared with: 4  $\mu\text{L}$  of GoTaq buffer 1X, 0.4  $\mu\text{L}$  dNTP at a final concentration of 0.2 mM each,  
203 1  $\mu\text{L}$  of each primer at a final concentration of 0.5  $\mu\text{M}$ , 0.1  $\mu\text{L}$  of GoTaq DNA polymerase 1.25  
204 U (Promega, city), 12.5  $\mu\text{L}$  of molecular-grade water, and 1  $\mu\text{L}$  of bacterial DNA for a final

205 volume of 20  $\mu\text{L}$  per reaction. The PCR reaction was carried out according to the following  
206 program: initial denaturation for 2 min at 95  $^{\circ}\text{C}$ , 30 cycles of 30 seconds at 95  $^{\circ}\text{C}$  for  
207 denaturation, 45 seconds at 55  $^{\circ}\text{C}$  for hybridization, and 1 minute at 72  $^{\circ}\text{C}$  for extension,  
208 followed by a final extension step of 4 minutes at 72  $^{\circ}\text{C}$ . The resulting amplicons were then  
209 purified using 2  $\mu\text{L}$  of Exosap-IT Express added to 5  $\mu\text{L}$  of each PCR product. The mixture  
210 was incubated for 4 minutes at 37  $^{\circ}\text{C}$ , followed by 1 minute at 80  $^{\circ}\text{C}$ . The 8F primer was used  
211 for sequencing a partial sequence of the 16S rDNA using the Sanger approach (subcontracting  
212 by Eurofins Genomics). The quality of the obtained electropherograms was verified using the  
213 Bioedit software (Hall, 1999). Sequences were compared to the GenBank database of the  
214 National Center for Biotechnology Information (NCBI) using the BLAST search algorithm to  
215 identify their taxonomy. For each sequence, all hits with a sequence coverage greater than 99%,  
216 a sequence identity greater than 97%, and an E-value of 0 were retained. The strain identified  
217 as *Ateromonas macleodii*, isolated from the inhibition zone, was then tested at different cell  
218 concentrations ( $10^6$ ,  $10^7$ ,  $10^8$  cells.mL<sup>-1</sup>) against targeted microalgae strains to check for  
219 potential growth inhibition using the same diffusion test protocol as described in the previous  
220 paragraph.

221

## 222 **Identification of the bacterial community in the biofilm**

223 To identify the bacterial community from the biofilm of the experimental culture system, we  
224 further used a metabarcoding approach on the samples from the bottom of the tank on March  
225 24 (14T) and July 19 2023 (131T), and from the roller fabric on the same date (131R). DNA  
226 was extracted from the 3 biofilm samples using the DNeasy PowerBiofilm Kit (Qiagen). The  
227 V3-V4 variable region of the 16S rRNA gene was amplified using a primer set designed to  
228 avoid the amplification of chloroplastic 16S rRNA gene: S-D-Bact-0341-b-S-17:  
229 CCTACGGGNGGCWGCAG as forward and 799F\_rc: CMGGGTATCTAATCCKGTT as  
230 reverse (Klindworth et al. 2013; Thomas et al. 2020). The PCR reaction mix was composed of  
231 12,5 $\mu\text{L}$  of KAPA HiFi HotStart ReadyMix 2X (KapaBiosystems), 0.75  $\mu\text{L}$  of each primer at a  
232 final concentration of 0.3  $\mu\text{M}$ , 9  $\mu\text{L}$  of molecular-grade water, and 2  $\mu\text{L}$  of bacterial DNA (2ng  
233  $\mu\text{L}^{-1}$ ) for a final volume of 25  $\mu\text{L}$  per reaction. PCR were carried out using the following  
234 program: initial denaturation for 3 min at 95  $^{\circ}\text{C}$ , 10 cycles of [30 s at 95  $^{\circ}\text{C}$ , 45 s at 44  $^{\circ}\text{C}$ , and  
235 90 s at 68  $^{\circ}\text{C}$ ], and 15 cycles of [20 s at 94  $^{\circ}\text{C}$ , 45 s at 50  $^{\circ}\text{C}$ , and 90 s at 68  $^{\circ}\text{C}$ ], followed by a  
236 final extension step of 4 min at 68  $^{\circ}\text{C}$ . Negative controls were used for the sampling, DNA  
237 extraction and PCR steps to control for potential contaminants. PCR were performed in  
238 triplicate and then pooled before metabarcoding. Amplicons were then sent to the GeT-

239 Biopuces platform for index addition, MiSeq Illumina sequencing (Run MiSeq 600 cycles V3)  
240 and sequence processing using the dada2 package (Callahan et al. 2016) in R (R Core Team,  
241 2021). Sequence processing included removal of sequences with N, of low quality and of size  
242 below 100 bp, and filtration of the phiX sequences. It also included sequence dereplication,  
243 ASV formation and chimera removal. Taxonomic annotation was done using Silva version  
244 v138.1 (Quast et al. 2013) and GTDB r202 (Parks et al. 2022). Before further analyses, the  
245 ASV table was transformed by normalizing the number of sequences using median sequencing  
246 depth (Trefault et al. 2021).

247

## 248 **Results**

249

### 250 **Algal inhibition from *Cylindrotheca closterium* biofilm**

251

252 A zone of inhibition was observed from the one-week *C. closterium* biofilm collected at the  
253 bottom of the tank, on the algal targets *N. oculata* and *T. striata* (Fig. 3). The percentages of  
254 inhibition relative to the positive control (hydrogen peroxide) for *N. oculata* and *T. striata*  
255 varied respectively between 65 to 158% and between 24 and 92%, according to the type of  
256 biofilm sample (i.e. pellet, supernatant, or whole) and days of experiment (Table 1). A  
257 percentage greater than 100% indicates that the observed inhibition area exceeds that of the  
258 positive control. However, no zone of inhibition was observed for the target *P. purpureum* for  
259 the three types of biofilm sample. Zones of inhibition on the *N. oculata* and *T. striata* targets  
260 was also observed when *C. closterium* grown on fabric was used as emitter. The percentages  
261 of inhibition relative to the positive control for *N. oculata* and *T. striata* varied respectively  
262 between 16 to 39% and between 12 to 38%, according to the three types of biofilm sample  
263 (Table 1). These inhibition activities seemed to be lower than that measured using the bottom  
264 tank biofilm (Table 1). No inhibition was observed on these targeted algal strains when filtered  
265 (0.2  $\mu\text{m}$ ) centrifuged biofilm supernatant was used.

266 Samples were taken from the diffusion tests in the inhibition zones and observed under  
267 an inverted microscope (Suppl. Fig. 1). Regarding the targeted microalgae *N. oculata*, we  
268 observed the presence of *C. closterium* cells in the samples taken from the inhibition zone of  
269 the paste, the pellet, and the supernatant. This observation suggests that the supernatant was not  
270 cell-free, as no *C. closterium* was detected when using 0.2  $\mu\text{m}$  filtered supernatant. We  
271 conclude that the centrifugation was not strong enough to pellet all *C. closterium* cells. From  
272 the inhibition zones of the supernatant from the *C. closterium* biofilm collected at the bottom

273 of the tank sampled after 14 days of experiment, different sizes of *N. oculata* cells were  
274 measured compared to *N. oculata* cultivated without any discs (control culture). In this  
275 inhibition zone, one population of *N. oculata* with cell diameters significantly larger than the  
276 control culture (Mann Whitney, n=20,  $p$ -value < 0.05) was observed with an average size of  
277  $5.1 \pm 0.7 \mu\text{m}$  (Table 2). A second population of *N. oculata* was also observed with cells  
278 significantly smaller than the control culture (Mann Whitney, n=20,  $p$ -value < 0.05) with an  
279 average size of  $1.8 \pm 0.8 \mu\text{m}$  (Table 2). In comparison, *N. oculata* population in the control  
280 culture had an average cell diameter of  $2.9 \pm 0.6 \mu\text{m}$  (Table 2). In this inhibition zone, we did  
281 not observe a significant change (Mann Whitney, n=20,  $p$ -value > 0.05, Table 2) in the length  
282 of *C. closterium* cells ( $50.9 \pm 2.3 \mu\text{m}$ ) in comparison to the *C. closterium* control, i.e. *C.*  
283 *closterium* growing alone on Petri dish ( $51.6 \pm 1.6 \mu\text{m}$ ). However, we observed a significant  
284 decrease in the width of the *C. closterium* cells, with a width of  $5.7 \pm 0.8 \mu\text{m}$  for the control  
285 culture and  $4.2 \pm 0.9 \mu\text{m}$  for the samples taken from the inhibition zone (Mann Whitney, n=20,  
286  $p$ -value < 0.05, Table 2). Regarding the targeted microalgae *T. striata*, we also observed the  
287 presence of *C. closterium* in the inhibition zone of the paste, the pellet, and the supernatant.  
288 When compared to the culture control (Figure 4), *T. striata* cells exhibited various cell size and  
289 shapes with visibly abnormal cells similar to those observed in positive control (35% hydrogen  
290 peroxide). In the inhibition zone of the supernatant from the *C. closterium* biofilm collected at  
291 the bottom of the tank sampled after 14 days of experiment, two types of *T. striata* cells were  
292 measured. One type was observed (Table 2) with an average diameter of  $11.1 \pm 1.2 \mu\text{m}$ , similar  
293 to the diameter of the control culture ( $10.9 \pm 1.4 \mu\text{m}$ , Mann Whitney, n=20,  $p$ -value > 0.05),  
294 and a second type of cells was observed with a significantly smaller average diameter of  $4.6 \pm$   
295  $0.7 \mu\text{m}$  (Mann Whitney, n=20,  $p$ -value < 0.05). As observed in the *N. oculata* inhibition zone,  
296 a change in the width of *C. closterium* cells in the *T. striata* inhibition zone of the supernatant  
297 from the *C. closterium* biofilm collected at the bottom of the tank sampled after 14 days of  
298 experiment, was measured (Table 2). In this inhibition zone, *C. closterium* cells had a diameter  
299 of  $3.8 \pm 0.7 \mu\text{m}$  (Table 2), which was significantly smaller than that of the control culture (Mann  
300 Whitney, n=20,  $p$ -value < 0.05). No change in cell diameter or number of *P. purpureum* was  
301 observed when growing in Petri dishes with or without *C. closterium* as emitter (Table 2).  
302 However, a significant difference in the width of *C. closterium* cells was also observed when  
303 co-cultured with *P. purpureum* vs. when cultured-alone (Mann–Whitney, n=20,  $p$ -value < 0.05,  
304 Table 2).

305

306 **Bacterial strains isolated from *Nannochloropsis oculata* and *Tetraselmis striata* inhibition**  
307 **zones**

308

309 Six bacterial strains were identified using a Sanger approach, after isolation from the inhibition  
310 zones of *T. striata* and *N. oculata*, showing mainly small white colonies (Table 3, Suppl. Table  
311 2). In the inhibition zones of *N. oculata*, isolated bacteria were assigned to the genus  
312 *Alteromonas* sp. (sequence coverage = 100%, sequence identity = 98.96%), and to the species  
313 *Alteromonas macleodii* (s.c. = 100%, s.i. = 98.02%). In the inhibition zones of *T. striata*,  
314 isolated bacteria were identified as the species *Alteromonas macleodii* (s.c. = 98.09 and  
315 96.86%, s.i. = 100 and 99% respectively), as well as the genus *Lacimonas* sp (s.c. = 96.97%,  
316 s.i. = 99%). The bacterial strain *A. macleodii* isolated from the inhibition zone of the centrifuged  
317 *C. closterium* biofilm supernatant was tested as a potential contributor of the inhibitory effect  
318 observed. However, no inhibition zone was clearly observed when the bacterial strain *A.*  
319 *macleodii* was tested alone against *N. oculata* and *T. striata*. .

320

321 **The bacterial community associated with *C. closterium* biofilm**

322 The metabarcoding analysis indicated that the three samples were composed of the classes:  
323 *Alphaproteobacteria*, *Bacteroidia*, and *Gammaproteobacteria*. *Alphaproteobacteria*  
324 dominated all samples with 97.3%, 87.5%, and 69.9% sequences from the one-week biofilm  
325 collected at the bottom of the tank after 14 days (March 24<sup>th</sup> 2023, referenced as 14T) and 131  
326 days of experiment (July 19<sup>th</sup> 2023, referenced as 131T), and from the three-week biofilm  
327 collected on the fabric of the roller after 131 days of experiment (July 19<sup>th</sup> 2023, referenced as  
328 131R), respectively (Figure 5, Suppl. Table 3). *Bacteroidia* and *Gammaproteobacteria* were  
329 similarly abundant in 14T with about 1% sequences. These two classes were also similarly  
330 abundant in 131T with about 6% sequences. *Gammaproteobacteria*, however, represented  
331 more sequences than *Bacteroidia* in 131R, with 26.1% and 3.9% sequences, respectively.  
332 Among *Alphaproteobacteria*, the genus *Roseinatronobacter* dominated the three samples with  
333 80.7%, 56.4%, and 50.9% sequences for 14T, 131R and 131T. Other genera included *Marivita*,  
334 *Oceanicaulis*, *Salinarimonas*, and a *Rhodobacteraceae* ASV, with *Marivita* and *Oceanicaulis*  
335 similarly abundant in 131R with about 10% sequences, *Rhodobacteraceae* ASV more abundant  
336 than the two genera in 14T with 13.6% sequences and *Salinarimonas* less abundant with 0.9-  
337 2.6% sequences. In *Gammaproteobacteria*, *Marinobacter* dominated all samples with 1.3%,  
338 4.5%, and 23.7% sequences in 14T, 131T, and 131R. Less abundant genera included  
339 *Congregibacter* and *Vibrio*, as well as *Alteromonas*, which was only present in 131T. Finally,

340 within *Bacteroidia*, *Phaeodactylibacter* was the most abundant in the samples, with 0.8%,  
341 4.6%, and 1.7% sequences respectively in 14T, 131T and 131R. Other *Bacteroidia* included  
342 *Muricauda* and the *Schleiferiaceae* UBA7878.

343

344

## 345 **Discussion**

346 Based on inhibition tests conducted using the biofilm of *Cylindrotheca closterium* as the  
347 emitter, the growth of the two targeted microalgae strains *Nannochloropsis oculata* and  
348 *Tetraselmis striata* was suppressed and resulted in change of cell size and shape. This finding  
349 represents evidence of growth inhibition observed among microalgae cultivated in biofilm co-  
350 cultures. Xu et al. (2019) reported previously that the cell-free filtrates of diatom *C. closterium*  
351 significantly reduced the growth of the dinoflagellate *Prorocentrum donghaiense* in planktonic  
352 cocultures. They showed that the extracts derived from the extracellular compounds of *C.*  
353 *closterium* affected the total chlorophyll content and therefore the efficiency of photosystem II  
354 of *P. donghaiense* cells. This led to the inhibition of photosynthesis and to the reduction in  
355 growth rate of this dinoflagellate species. Similarly, allelopathic activities were evidenced from  
356 other diatom species on various algal target strains using planktonic co-cultures from living  
357 cells, culture filtrates, and filtrate or cell extracts (Sholz and Liebezeit 2012, Xu et al 2015,  
358 Wang et al 2016). In the present study, we observed an effect of *C. closterium* biofilm on cell  
359 diameter of *N. oculata* as well as of *T. striata*, where cells exhibited various size and shape.  
360 Other studies have also reported morphological alterations due to an allelopathic effect. For  
361 example, Pichierri et al. (2017) observed *Ostreopsis cf. ovata* cells with abnormal morphologies  
362 when exposed to the individual acellular filtrate from two diatoms species (*Proschkinia*  
363 *complanatoides* and *Navicula* sp.), including membrane deformations and deleterious effects  
364 on the nucleus, resulting in chromatin dispersion in the cytoplasm. However, in the present  
365 study, no inhibition effect was observed from *C. closterium* the filtered biofilm supernatant at  
366 0.2  $\mu\text{m}$ , thus without bacteria or microalgae. This suggests that compounds leading to the  
367 inhibition or death and the cell deformation of targeted algal strains were highly labile or a  
368 physical contact is required between *C. closterium* biofilm and the targets. These compounds  
369 appeared to exhibit a limited bioactive duration, likely necessitating continuous production and  
370 release during diatom cell growth or direct contact with targeted cells to optimize their  
371 efficiency The biofilm of *C. closterium* may have been able to produce metabolites, such as  
372 observed with other microalgae (Zhao et al. 2019, Long et al. 2021) capable of altering  
373 chlorophyll pigment or cytoplasmic membranes, and thereby inhibiting photosystem II, which

374 directly impacts photosynthesis functioning. This impact on photosynthesis would lead to  
375 modifications in the cell cycle, division, and growth of the targeted microalgae, and this would  
376 explain the appearance of various morphotypes. Furthermore, we observed in our study a  
377 significant reduction of the width of *C. closterium* cells growing in the inhibition areas, which  
378 was not observed to date in studies investigating the allelochemical potential of this diatom.  
379 The reduction in cell width due to mitotic division is unlikely, as no decrease in cell length was  
380 observed, contrasting with the commonly reported size reduction in daughter cells following  
381 vegetative division in pennate diatoms (Macdonald 1869, Pfitzer 1869). Nonetheless, several  
382 studies reported a decrease in cell width of *C. closterium* and other pennate diatoms, along with  
383 a reduction in growth rate, in response to environmental stresses such as silica or iron limitation  
384 (Georges et al 2022, Marchetti and Harrison 2007). This response was interpreted as a reduction  
385 of frustule thickness or an increase of the surface-to-volume ratio facilitating micronutrient  
386 diffusion into the cells. We could therefore hypothesize that the production of inhibitory  
387 molecules by the *C. closterium* biofilm represents a substantial metabolic cost, leading to a  
388 slower growth of the diatom (Legrand et al. 2003, Allen et al. 2016). This may also result in a  
389 reduction in cell width, which could facilitate the release of allelochemical molecules through  
390 passive diffusion.

391 In the present study, no inhibition was observed for *Porphyridium purpureum*, a benthic  
392 microalga. The discrimination of inhibitory compounds on the target could be related to the  
393 physiology of this microalgae that possesses sulfated polysaccharide cell wall exhibiting strong  
394 antioxidant activity (Tannin-Spitz et al. 2005). This ability may protect cells against the  
395 potential damaging effects of reactive oxygen species (ROS) triggering oxidative stress under  
396 the stimulation of allelochemicals. Indeed, antialgal substances from *C. closterium* have been  
397 suggested to provoke oxidative stress on the dinoflagellate *P. donghaiense* (Xu et al. 2019).  
398 The bacterial strain *Alteromonas macleodii* isolated from the inhibition zone of centrifuged *T.*  
399 *striata* supernatant did not show any significant antialgal activity. As *Cylindrotheca*'s biofilm  
400 and the cultures from the targeted microalga *T. striata* were not axenic, the isolated bacterial  
401 strains could come from either of them. In the case where *A. macleodii* came from the biofilm,  
402 it was not involved in the antialgal activity while in the case where it came from *Tetraselmis*  
403 *striata* culture, it was likely living in association with the algae. Like several  
404 *Gammaproteobacteria*, bacteria belonging to the genus *Alteromonas* are often found living in  
405 association with microalgae (Grossart et al. 2005, Sapp et al. 2007), such as *N. oculata*  
406 (Chernikova et al. 2020) or as competitors of *T. suecica* for nutrients (Biondi et al. 2017). The  
407 bacterial community survey of the biofilm from the tank and the roller indicated that

408 *Alteromonas* was present in only one sample and in low sequence numbers. *Alteromonas*  
409 *macleodii* may form short-lived ‘blooms’ of active cells that are missed using traditional single-  
410 point sampling (Wietz et al. 2022). Another hypothesis could be that the isolated strain came  
411 from one of the targeted cultures instead of the *C. closterium* biofilm. The bacterial community  
412 from the one-week biofilms of the tank and the three-week biofilm of the roller fabric also  
413 contained a large majority of *Alphaproteobacteria* with the genus *Roseinatronobacter*  
414 dominating in all samples. Bacteria from the genus *Roseinatronobacter* are facultatively  
415 phototrophic purple bacteria, found in environments characterized as extreme such as  
416 alkaliphilic hypersaline lakes and are highly tolerant to large environmental gradient variations  
417 (Boldareva et al. 2007, Wilson et al. 2012, Trutschel et al. 2023, Cubillos et al. 2024). Such  
418 large variations likely happen in our rotating system where bacteria are impacted in the biofilm  
419 by varying humidity conditions and salt concentrations due to evaporation. The other  
420 *Alphaproteobacteria* genera, *Marivita*, *Oceanicaulis*, and *Salinarimonas* have previously been  
421 observed associated with algal planktonic cultures or in algal biofilms and are believed to play  
422 a role in nutrient transformation and availability to the algae (Zhou et al. 2021, Lukwambe et  
423 al. 2023, Li et al. 2019, Cole et al. 2014, Strömpl et al. 2003). For instance, *Salinarimonas* has  
424 been shown to promote algal growth in the biofilm (Xiao et al. 2023). Within  
425 *Gammaproteobacteria*, *Marinobacter* has been identified in association with the phycosphere  
426 or the biofilm of microalgae, likely benefiting from carbon source exudates and its cells have  
427 been shown to be chemically attracted by the diatom *Thalassiosira weissflogii* (Giraldo et al.  
428 2019, Pinto et al. 2021, Sonnenschein et al. 2012). Within *Bacteroidia*, *Muricauda*, is a genus  
429 regularly found in biofilms and thought to be, as well as the genus *Marinobacter*, amongst the  
430 primary colonizers, and bacteria from this genus have been shown to play a role in cell  
431 aggregation of the microalgae *Nannochloropsis oceanica* (Abed et al. 2019, Wang et al. 2012).  
432 *Phaeodactylibacter* bacteria are heterotrophic denitrifiers and salt tolerant, they are found in  
433 biofilms and associated with microalgae such as the diatom *Phaeodactylum tricorutum* (Chen  
434 et al. 2014, Li et al. 2021, Wang et al. 2020, Fan et al. 2023). Overall, the bacterial community  
435 associated with *C. closterium* biofilm contains genera that could play various roles such as  
436 making complex molecules available to the algae, cell aggregation or with various osmotic  
437 properties. Although the main bacterial strain isolated from the inhibition areas did not  
438 participate directly in the targeted microalgae inhibition, bacteria closely associated with *C.*  
439 *closterium* biofilm could have a role in the observed inhibition activity.

440 In conclusion, this study demonstrates the allelopathic potential of *Cylindrotheca*  
441 *closterium* growing in biofilms inhibiting the growth of two targeted microalgal species,

442 *Nannochloropsis oculata* and *Tetraselmis striata*. The observed inhibition appears to be linked  
443 to compounds produced either by the growing diatom or its associated bacterial community.  
444 Additional experiments may include omics tools such as metabolomics or metatranscriptomics  
445 to identify allelochemical compounds and the metabolic pathways of the biofilm microbiota  
446 involved in algal growth inhibition. Additionally, the results highlight the potential of such  
447 allelopathic interactions in enhancing microalgal cultivation by suppressing competitors,  
448 making *C. closterium* a candidate for developing more efficient and contamination-resistant  
449 algal biofilm technologies. However, further experiments are necessary to broaden the  
450 spectrum of algal targets and fully characterize the bioactive compounds and their effects.

451

452

453

454

455

#### 456 **Funding**

457 This work was supported by the Photobiofilm Explorer project ANR-20-CE43-0008.

458

#### 459 **Competing interests**

460 The authors declare no conflict of interest.

461

#### 462 **Availability of data**

463 Partial 16S rRNA gene sequences were deposited in GenBank under the Accession number  
464 PP551695-PP551700. Raw 16S rRNA gene sequences and sample metadata are available in  
465 the SRA under BioProject ID PRJNA1098477.

466

#### 467 **Authors' contributions**

468 Conceptualization: Emilie Le Floc'h, Eric Fouilland; Methodology: Lucie Sanchez, Amandine  
469 Avouac, Emilie Le Floc'h, Christine Félix, Christophe Leboulanger, Angélique Gobet ; Formal  
470 analysis and investigation: Lucie Sanchez, Emilie Le Floc'h, Christine Félix, Angélique  
471 Gobet ; Validation: Lucie Sanchez, Emilie Le Floc'h, Christine Félix, Eric Fouilland ;  
472 Visualization : Lucie Sanchez, Emilie Le Floc'h, Angélique Gobet, Eric Fouilland ; Writing-  
473 original draft preparation: Lucie Sanchez, Eric Fouilland ; Writing- review and editing: Lucie  
474 Sanchez, Amandine Avouac, Emilie Le Floc'h, Christine Félix, Christophe Leboulanger,  
475 Angélique Gobet, Eric Fouilland ; Supervision ; Emilie Le Floc'h, Christine Félix, Eric

476 Fouilland; Funding acquisition and project administration: Eric Fouilland ; Ressources :  
477 Amandine Avouac, Emilie Le Floc’h, Christine Félix

478

#### 479 **Acknowledgments**

480 We thank the GeT-Biopuces platform, TBI (Université de Toulouse, CNRS, INRAE, INSA)  
481 and especially Lidwine Trouilh for MiSeq sequencing and Etienne Rifa for sequence  
482 processing. We also thank Eric Pruvost from LOV laboratory in Villefranche-sur-Mer, France,  
483 for providing the design of the experimental rotating system used in the present study.

484

#### 485 **References**

486

487 Abed RMM, Al Fahdi D, Muthukrishnan T (2019) Short-term succession of marine microbial  
488 fouling communities and the identification of primary and secondary colonizers.  
489 *Biofouling* 35: 526-540.

490 Allen JL, Ten-Hage L, Leflaive J (2016) Allelopathic interactions involving benthic  
491 phototrophic microorganisms. *Env Microbiol Rep* 8: 752–762

492 Biondi N, Cheloni G, Rodolfi L, Viti C, Giovannetti L, Tredici MR (2018) *Tetraselmis suecica*  
493 F&M-M33 growth is influenced by its associated bacteria. *Microb Biotechnol* 11:211-  
494 223.

495 Boldareva EN, Briantseva IA, Tsapin A, Nelson K, Sorokin DI, Turova TP, Boichenko VA,  
496 Stadnichuk IN, Gorlenko VM (2007) The new alkaliphilic bacteriochlorophyll a-  
497 containing bacterium *Roseinatronobacter monicus* sp. nov. from the hypersaline Soda  
498 Mono Lake (California, United States). *Mikrobiologiya* 76: 82–92.

499 Callahan BJ, McMurdie PJ, Rosen MJ, Han AW, Johnson AJA, Holmes SP (2016). DADA2:  
500 High-resolution sample inference from Illumina amplicon data. *Nature Methods* 13: 581–  
501 583.

502 Chaïb S, Pistevos JCA, Bertrand C, Bonnard (2021) Allelopathy and allelochemicals from  
503 microalgae: An innovative source for bio-herbicidal compounds and biocontrol research.  
504 *Algal Res* 54: 102213

505 Chen Z, Lei X, Lai Q, Li Y, Zhang B, Zhang J, Zhang H, Yang L, Zheng W, Tian Y, Yu Z, Xu  
506 H, Zheng T (2014) *Phaeodactylibacter xiamenensis* gen. nov., sp. nov., a member of the  
507 family Saprospiraceae isolated from the marine alga *Phaeodactylum tricornutum*. *Int J*  
508 *Syst Evol Microbiol*, 64: 3496-3502.

509 Chernikova TN, Bargiela R, Toshchakov SV, Shivaraman V, Lunev EA, Yakimov MM,  
510 Thomas DN, Golyshin PN (2020) Hydrocarbon-Degrading Bacteria *Alcanivorax* and  
511 *Marinobacter* Associated With Microalgae *Pavlova lutheri* and *Nannochloropsis*  
512 *oculata*. Front Microbiol 11: 572931.

513 Cole JK, Hutchison JR, Renslow RS, Kim YM, Chrisler WB, Engelmann HE, Dohnalkova AC,  
514 Hu D, Metz TO, Fredrickson JK, Lindemann SR (2014) Phototrophic biofilm assembly  
515 in microbial-mat-derived unicyanobacterial consortia: model systems for the study of  
516 autotroph-heterotroph interactions. Front Microbiol 5: 109.

517 Coyne KJ, Wang Y, Johnson G (2022) Algicidal Bacteria: A Review of Current Knowledge  
518 and Applications to Control Harmful Algal Blooms. Front Microbiol 13: 871177.

519 Cubillos CF, Aguilar P, Moreira D, Bertolino P, Iniesto M, Dorador C, López-García P (2024)  
520 Exploring the prokaryote-eukaryote interplay in microbial mats from an Andean  
521 athalassohaline wetland. Microbiol Spectr 12: e0007224.

522 Donlan RM (2002) Biofilms: microbial life on surfaces. Emerg Infect Dis 8:881-90.

523 Edwards U, Rogall T, Blocker H, Emde M, Bottger EC (1989) Isolation and direct complete  
524 nucleotide determination of entire genes. Characterization of a gene coding for 16S  
525 ribosomal RNA. Nucl Acids Res 17:7843–7853.

526 Flores E, Wolk CP (1986) Production, by filamentous, nitrogen-fixing cyanobacteria, of a  
527 bacteriocin and of other antibiotics that kill related strains. Arch Microbiol 145: 215–219.

528 Flores HS, Wikfors GH, Dam HG (2012) Reactive oxygen species are linked to the toxicity of  
529 the dinoflagellate *Alexandrium* spp. to protists. Aquat Microb Ecol 66:199-209

530 Grossart H-P, Levold F, Allgaier M, Simon M, Brinkhoff T (2005) Marine diatom species  
531 harbor distinct bacterial communities. Environmental Microbiology 7: 860–873.

532 Fan G, Huang J, Jiang X, Meng W, Yang R, Guo J, Fang F, Yang J (2023) Microalgae biofilm  
533 photobioreactor and its combined process for long-term stable treatment of high-saline  
534 wastewater achieved high pollutant removal efficiency. Journal of Environmental  
535 Chemical Engineering 11: 111473.

536 Georges M, Bourguiba A, Boutouil M, Chateigner D, Jolly O, Claquin P (2022) Interaction  
537 between the diatom *Cylindrotheca closterium* and a siliceous mortar in a silica-limited  
538 environment. Construction and Building Materials 323: 126277.

539 Giraldo JB, Stock W, Dow L, Roef L, Willems A, Mangelinckx S, Kroth PG, Vyverman W,  
540 Michiels M (2019) Influence of the algal microbiome on biofouling during industrial  
541 cultivation of *Nannochloropsis* sp. in closed photobioreactors. Algal Research 42:  
542 101591.

543 Guillard RRL, Ryther JH (1962) Studies of marine planktonic diatoms. I. *Cyclotella nana*  
544 Hustedt and *Detonula confervacea* Cleve. Can J Microbiol 8: 229-239.

545 Guillard RRL (1975). Culture of phytoplankton for feeding marine invertebrates. In Smith WL  
546 and Chanley MH (Eds.) Culture of Marine Invertebrate Animals. Plenum Press, New  
547 York, USA, pp 26-60.

548 Gross EM (2003) Allelopathy of Aquatic Autotrophs. Crit Rev Plant Sci 22: 313-339

549 Inderjit, del Moral R (1997) Is separating resource competition from allelopathy realistic? The  
550 Botanical Review 63: 221–230

551 Hellio C, Berge JP, Beaupoil C, Le GAL Y, Bourgougnon N (2002). Screening of Marine  
552 Algal Extracts for Anti-settlement Activities against Microalgae and Macroalgae.  
553 Biofouling, 18: 205–215.

554 Hudzicki J (2009) Kirby-Bauer Disc Diffusion Susceptibility Test Protocol. American Society  
555 for Microbiology, Washington DC: Dec 8, 2009 posting date [Online.]

556 Khairy (2010) Allelopathic effects of *Skeletonema costatum* (Bacillariophyta) exometabolites  
557 on the growth of *Nannochloropsis oculata* and *Tetraselmis chuii* (Chlorophyta). Egypt.  
558 J Exp Biol (Bot) 6: 79-85.

559 Klindworth A, Pruesse E, Schweer T, Peplies J, Quast C, Horn M, Glöckner FO (2013)  
560 Evaluation of general 16S ribosomal RNA gene PCR primers for classical and next-  
561 generation sequencing-based diversity studies. Nucleic Acids Research 41: 1–11.

562 Leflaive J, Ten-Hage L (2007) Algal and Cyanobacterial Secondary Metabolites in  
563 Freshwaters: A Comparison of Allelopathic Compounds and Toxins. Fresh Biol 52: 199-  
564 214

565 Legrand C, Rengefors K, Fistarol GO and Granéli E (2003) Allelopathy in Phytoplankton -  
566 Biochemical, Ecological and Evolutionary Aspects. Phycologia 42: 406-419

567 Li J, Wang T, Yu S, Bai J, Qin S (2019) Community characteristics and ecological roles of  
568 bacterial biofilms associated with various algal settlements on coastal reefs. J Environ  
569 Manage 250: 109459.

570 Li Y, Wu Y, Wang S, Jia L (2021) Effect of organic loading on phosphorus forms  
571 transformation and microbial community in continuous-flow A2/O process. Water Sci  
572 Technol 83: 2640-2651.

573 Long M, Peltekis A, González-Fernández C, Hégaret H, Bailleul B (2021) Allelochemicals of  
574 *Alexandrium minutum*: Kinetics of membrane disruption and photosynthesis inhibition in  
575 a co-occurring diatom. Harmful Algae 103:101997.

576 Lukwambe B, Nicholous R, Zheng Z (2024) The functional diversity of microbial communities  
577 in the multi-compartment biofilters of shrimp mariculture effluents using 16S rRNA  
578 metabarcoding. *Aquacult Int* 32: 1081–1099.

579 MacDonald JD (1869). On the structure of the diatomaceous frustule, and its genetic cycle. *Ann*  
580 *Ma. Nat Hist* 4: 1–8.

581 Marchetti A, Harrison PJ (2007) Coupled changes in the cell morphology and the elemental (C,  
582 N, and Si) composition of the pennate diatom *Pseudo-nitzschia* due to iron deficiency.  
583 *Limnol Oceanogr* 52: 2270-2284.

584 Morales M, Bonnefond H, Bernard O (2020) Rotating algal biofilm versus planktonic  
585 cultivation: LCA perspective. *J Cleaner Prod* 254: 120547

586 Parks DH, Chuvochina M, Rinke C, Mussig AJ, Chaumeil P-A, Hugenholtz P (2022) GTDB:  
587 An ongoing census of bacterial and archaeal diversity through a phylogenetically  
588 consistent, rank normalized and complete genome-based taxonomy. *Nucleic Acids*  
589 *Research* 50: D785–D794.

590 Pascon G, Messina M, Petit L, Pinheiro Valente LM, Oliveira B, Przybyla C, Dutto G and Tulli  
591 F (2021) Potential application and beneficial effects of a marine microalgal biomass  
592 produced in a high-rate algal pond (HRAP) in diets of European sea bass, *Dicentrarchus*  
593 *labrax*. *Env Sci Pollut Res* 28: 62185–62199

594 Penaranda D, Bonnefond H, Guihéneuf F, Morales M, Bernard O (2023) Life cycle assessment  
595 of an innovative rotating biofilm technology for microalgae production: An eco-design  
596 approach. *J Cleaner Prod* 384: 135600

597 Pfitzer E (1869) Über den Bau und die Zelltheilung der Diatomeen. *Botanische Zeitung Berlin*  
598 27:774–776.

599 Pichierri S, Accoroni S, Pezzolesi L, Guerrini F, Romagnoli T, Pistocchi R, Totti C (2017)  
600 Allelopathic effects of diatom filtrates on the toxic benthic dinoflagellate *Ostreopsis* cf.  
601 *ovata*. *Mar Environ Res* 131:116-122.

602 Pinto J, Lami R, Krasovec M, Grimaud R, Urios L, Lupette J, Escande ML, Sanchez F,  
603 Intertaglia L, Grimsley N, Piganeau G, Sanchez-Brosseau S (2021) Features of the  
604 Opportunistic Behaviour of the Marine Bacterium *Marinobacter algicola* in the  
605 Microalga *Ostreococcus tauri* Phycosphere. *Microorganisms* 9: 1777.

606 Quast C, Pruesse E, Yilmaz P, Gerken J, Schweer T, Yarza P, Peplies J, Glöckner FO (2013).  
607 The SILVA ribosomal RNA gene database project: Improved data processing and web-  
608 based tools. *Nucleic Acids Research* 41: 590–596.

609 R Core Team (2021) R: A Language and Environment for Statistical Computing. [http://www.r-](http://www.r-project.org/)  
610 [project.org/](http://www.r-project.org/)

611 Sapp M, Schwaderer AS, Wiltshire KH, Hoppe H-G, Gerdts G, Wichels A (2007) Species-  
612 specific bacterial communities in the phycosphere of microalgae. *Microbial Ecology* 53:  
613 683–699.

614 Scholz B, Liebezeit G (2012) Screening for competition effects and allelochemicals in  
615 benthic marine diatoms and cyanobacteria isolated from an intertidal flat (southern North  
616 Sea). *Phycologia* 51 4:432-450

617 Sonnenschein EC, Syit DA, Grossart HP, Ullrich MS (2012) Chemotaxis of *Marinobacter*  
618 *adhaerens* and its impact on attachment to the diatom *Thalassiosira weissflogii*. *Appl*  
619 *Environ Microbiol* 78: 6900-7.

620 Stackebrandt E, Liesack W (1993) Nucleic acids and classification. In: Handbook of new  
621 bacterial systematics, pp. 151- 194. Academic Press Ltd., London.

622 Strömpl C, Hold GL, Lünsdorf H, Graham J, Gallacher S, Abraham WR, Moore ER, Timmis  
623 KN (2003) *Oceanicaulis alexandrii* gen. nov., sp. nov., a novel stalked bacterium isolated  
624 from a culture of the dinoflagellate *Alexandrium tamarense* (Lebour) Balech. *Int J Syst*  
625 *Evol Microbiol* 53:1901-6.

626 Tannin-Spitz T, Bergman M, van Moppes D, Grossman S, Arad SM (2005) Antioxidant activity  
627 of the polysaccharide of the red microalga *Porphyridium* sp. *J Appl Phycol* 17:215–222.

628 Thomas F, Dittami SM, Brunet M, Le Duff N, Tanguy G, Leblanc C, Gobet A (2020).  
629 Evaluation of a new primer combination to minimize plastid contamination in 16S rDNA  
630 metabarcoding analyses of alga-associated bacterial communities. *Environmental*  
631 *Microbiology Reports* 12: 30–37.

632 Trefault N, De La Iglesia R, Moreno-Pino M, Lopes Dos Santos A, Gérikas Ribeiro C, Parada-  
633 Pozo G, Cristi A, Marie D, Vaultot D (2021) Annual phytoplankton dynamics in coastal  
634 waters from Fildes Bay, Western Antarctic Peninsula. *Scientific Reports* 11: 1368.

635 Trutschel LR, Rowe AR, Sackett JD (2023) Complete genome sequence of *Roseinatronobacter*  
636 sp. strain S2, a chemolithoheterotroph isolated from a pH 12 serpentinizing system.  
637 *Microbiol Resour Announc* 12: e0028823.

638 Uchida T (2001) The role of cell contact in the life cycle of some dinoflagellate species. *J*  
639 *Plankton Res* 23: 889–891

640 Vallina SM, Follows MJ, Dutkiewicz S, Montoya JM, Cermeno P, Loreau M (2014) Global  
641 relationship between phytoplankton diversity and productivity in the ocean. *Nature*  
642 *Communications* 5: 4299

643 Wang H, Laughinghouse HD 4th, Anderson MA, Chen F, Williams E, Place AR, Zmora O,  
644 Zohar Y, Zheng T, Hill RT (2012) Novel bacterial isolate from Permian groundwater,  
645 capable of aggregating potential biofuel-producing microalga *Nannochloropsis oceanica*  
646 IMET1. *Appl Environ Microbiol* 78:1445-53.

647 Wang J, Zhou J, Wang Y, Wen Y, He L, He Q (2020) Efficient nitrogen removal in a modified  
648 sequencing batch biofilm reactor treating hypersaline mustard tuber wastewater: The  
649 potential multiple pathways and key microorganisms. *Water Res* 177: 115734.

650 Wang R, Wang J, Xue Q, Tan L, Cai J, Wang H (2016) Preliminary analysis of  
651 allelochemicals produced by the diatom *Phaeodactylum tricornutum*. *Chemosphere*  
652 165:298-303

653 Wietz M, López-Pérez M, Sher D, Biller SJ, Rodriguez-Valera F (2022) Microbe Profile:  
654 *Alteromonas macleodii* - a widespread, fast-responding, 'interactive' marine bacterium.  
655 *Microbiology (Reading)* 168: 001236.

656 Wenjing X, Wang J, Tan L, Guo X, Xue Q (2019) Variation in Allelopathy of Extracellular  
657 Compounds Produced by *Cylindrotheca Closterium* against the Harmful-Algal-Bloom  
658 Dinoflagellate *Prorocentrum Donghaiense*. *Mar Env Res* 148: 19-25

659 Wilson SL, Frazer C, Cumming BF, Nuin PA, Walker VK (2012) Cross-tolerance between  
660 osmotic and freeze-thaw stress in microbial assemblages from temperate lakes. *FEMS*  
661 *Microbiol Ecol* 82: 405-15.

662 Xiao C, Yuan J, Li L, Zhong N, Zhong D, Xie Q, Chang H, Xu Y, He X, Li M (2022)  
663 Photocatalytic synergistic biofilms enhance tetracycline degradation and conversion.  
664 *Environ Sci Ecotechnol* 4: 100234.

665 Xu N, Tang YZ, Qin J, Duan S, Gobler CJ (2015) Ability of the marine diatoms *Pseudo-*  
666 *nitzschia multiseriis* and *P. pungens* to inhibit the growth of co-occurring phytoplankton  
667 via allelopathy. *Aquat Microb Ecol* 74 1:29-41

668 Xu W, Tan L, Guo X, Wang J (2019) Isolation of anti-algal substances from *Cylindrotheca*  
669 *closterium* and their inhibition activity on bloom-forming *Prorocentrum donghaiense*.  
670 *Ecotox Environ Safety* 190: 110180

671 Zhao JX, Yang L, Zhou Lv, Bai Y, Wang B, Hou P, Xu Q, Yang W, Zuo Z (2019) Inhibitory  
672 effects of eucalyptol and limonene on the photosynthetic abilities in *Chlorella vulgaris*  
673 (Chlorophyceae). *Phycologia* 55: 696-702

674 Zhou X, Zhang XA, Jiang ZW, Yang X, Zhang XL, Yang Q (2021) Combined characterization  
675 of a new member of *Marivita cryptomonadis* strain LZ-15-2 isolated from cultivable

676 phycosphere microbiota of highly toxic HAB dinoflagellate *Alexandrium catenella*  
677 LZT09. Braz J Microbiol 52: 739–748.  
678

679 **Tables**

680

681 Table 1: Results obtained of the inhibition test conducted after 15 days of incubation under  
 682 continuous light with *Nannochloropsis oculata*, *Tetraselmis striata* and *Porphyridium*  
 683 *purpureum* as the targeted microalgae strain and *Cyclindrotheca closterium* in biofilm  
 684 (harvested from the bottom of the tank or from the fabric of the roller) acting as the emitter  
 685 when (i) the whole biofilm, (ii) the centrifuged biofilm pellet, and (iii) the centrifuged biofilm  
 686 supernatant filtered or not, incubated after 14 and 131 days of experiment using the rotating  
 687 system. Results are expressed as the percentage (%) of the inhibition zone measured around the  
 688 diffusion discs with the emitter relative to the inhibition zone measured with hydrogen peroxide  
 689 as the positive control. Mean and range from replicates (n=2) are reported.

Days of Experiment	Target species	One-week old biofilm from the bottom of the tank			Three-week old biofilm from the roller fabric			
		Whole biofilm	centrifuged biofilm pellet	centrifuged biofilm supernatant	Whole biofilm	centrifuged biofilm pellet	centrifuged biofilm supernatant	filtered centrifuged biofilm supernatant
14 days (March 24th 2023)	<i>N. oculata</i>	150 (±16)	91 (±60)	158 (±43)	not tested	not tested	not tested	not tested
	<i>T. striata</i>	33 (±5)	24 (±10)	33 (±2)	not tested	not tested	not tested	not tested
	<i>P. purpureum</i>	0	0	0	not tested	not tested	not tested	not tested
131 days (July 19th 2023)	<i>N. oculata</i>	65 (±21)	not tested	not tested	39 (±10)	16 (±4)	26 (±26)	0
	<i>T. striata</i>	92 (±19)	not tested	not tested	12 (±6)	18 (±18)	38 (±14)	0
	<i>P. purpureum</i>	0	not tested	not tested	0	0	0	0

690

691

692

693 Table 2: Cell size (length, width, or diameter in  $\mu\text{m}$ ) of *Cyclindrotheca closterium* and targeted  
 694 strains *Nannochloropsis oculata*, *Tetraselmis striata* and *Porphyridium purpureum*, measured  
 695 in culture grown alone (negative control) and in zones around discs containing supernatant from  
 696 the one-week *C. closterium* biofilm (collected from the bottom of the tank on March 19<sup>th</sup> 2023).  
 697 Sampling occurred after 14 days of experiment. Mean and standard deviation from replicates  
 698 (n=20) are reported. A and B represent strains from the same species but with different cell  
 699 size.

Observation zone	Observed strains				
	<i>C. closterium</i>		<i>T. striata</i>	<i>N. oculata</i>	<i>P. purpureum</i>
	length	width	diameter	diameter	diameter
strain cultivated alone (= negative control)	51.6 $\pm$ 1.6	5.7 $\pm$ 0.8	10.9 $\pm$ 1.4	2.9 $\pm$ 0.6	5.5 $\pm$ 1.2
<i>T. striata</i> Inhibition Zone	51.2 $\pm$ 1.5	3.8 $\pm$ 0.7	A: 11.1 $\pm$ 1.2	-	-
			B: 4.6 $\pm$ 0.7	-	-
<i>N. oculata</i> Inhibition Zone	50.9 $\pm$ 2.3	4.2 $\pm$ 0.9	-	A: 5.1 $\pm$ 0.7	-
			-	B: 1.8 $\pm$ 0.8	-
<i>P. purpureum</i> Coexistence Zone	50.3 $\pm$ 1.6	4.4 $\pm$ 0.8	-	-	5.2 $\pm$ 0.9

700

701

702

703 Table 3. Identification of bacterial colonies isolated from inhibition zones of the targeted  
 704 microalgae around the biofilm type, from the one-week biofilm growing at bottom of the tank  
 705 collected on March 19<sup>th</sup> 2023. Details on sequence taxonomic identification are available in  
 706 Supplementary Table 2.

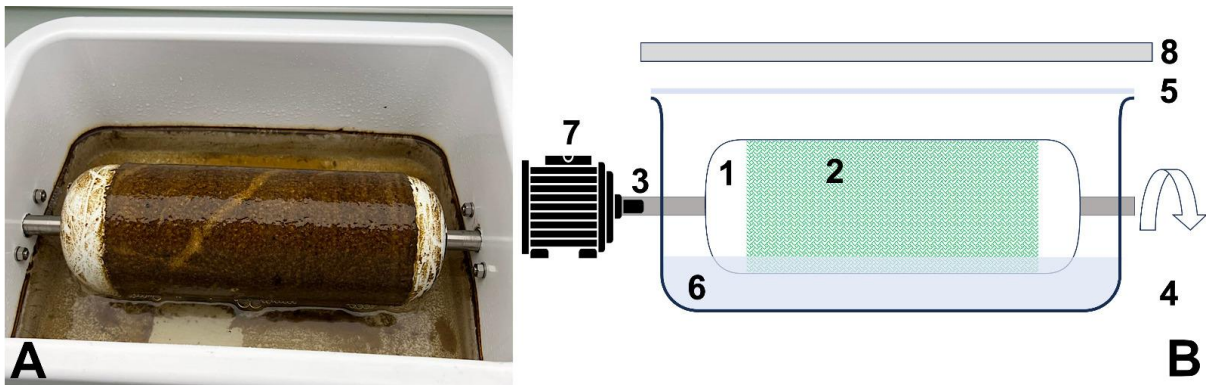
Inhibition zone from the targeted microalga	Putative bacterial species	16S rDNA sequence length (bp)	Sequence coverage (%)	Sequence identity (%)	Accession number of the best hit	
centrifuged biofilm supernatant	<i>Alteromonas macleodii</i>	858	100%	98.02%	MT325885.1	
<i>N. oculata</i>	whole biofilm	<i>Alteromonas</i> sp.	1094	100%	98.17%	MT210817.1
	whole biofilm	<i>Alteromonas</i> sp.	772	100%	98.96%	MF599947.1
centrifuged biofilm supernatant	<i>Alteromonas macleodii</i>	941	100%	98.09%	MT325885.1	
<i>T. striata</i>	whole biofilm	<i>Alteromonas macleodii</i>	834	99%	96.86%	HM584088.1
	whole biofilm	<i>Lacimonas</i> sp.	860	99%	96.97%	MK493541.1

707

708

709

710



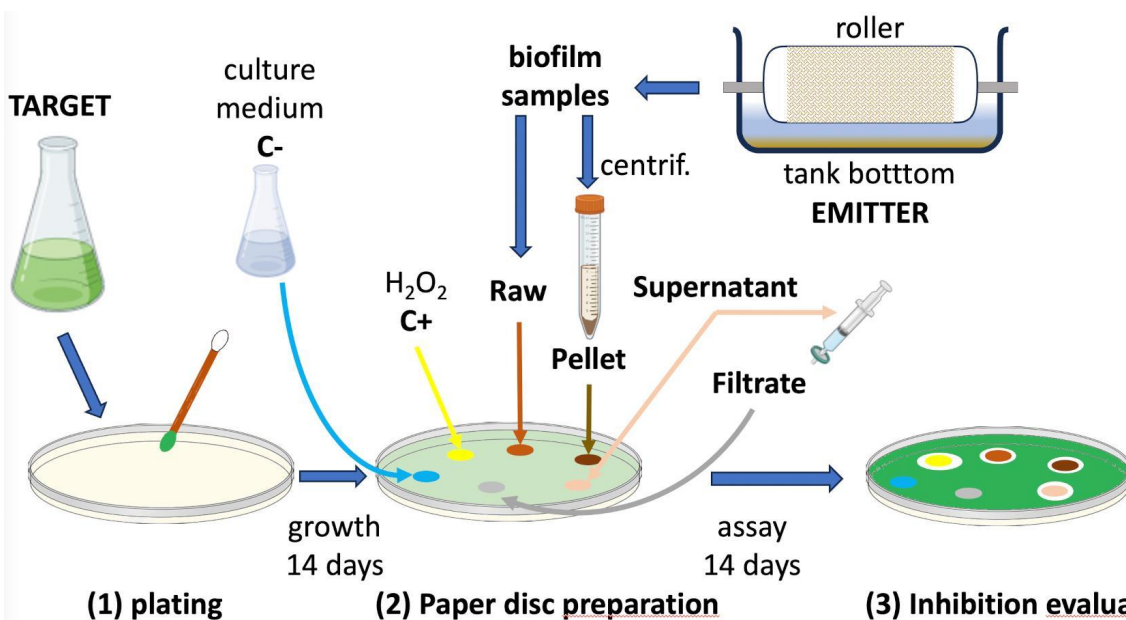
711

712 Figure 1: A: Macroscopic view of *Cyldrotheca closterium* growing as biofilm. B:  
713 Experimental rotating culture system. 1: cylindrical fender (10 cm diameter, 28 cm length); 2:  
714 22x31 cm cotton fabric; 3: stainless steel axis; 4 : white HDPE tank 34\*24\*16 (L\*1\*H) cm  
715 internal; 5 : 4 mm thick acrylic cover; 6: 3.6 L of f/2 medium with double N and P supply; 7: 5  
716 to 40 rpm variable speed motor with driver; 8: dimmable 130\*40 cm 40 W LED panel.

717

718

719



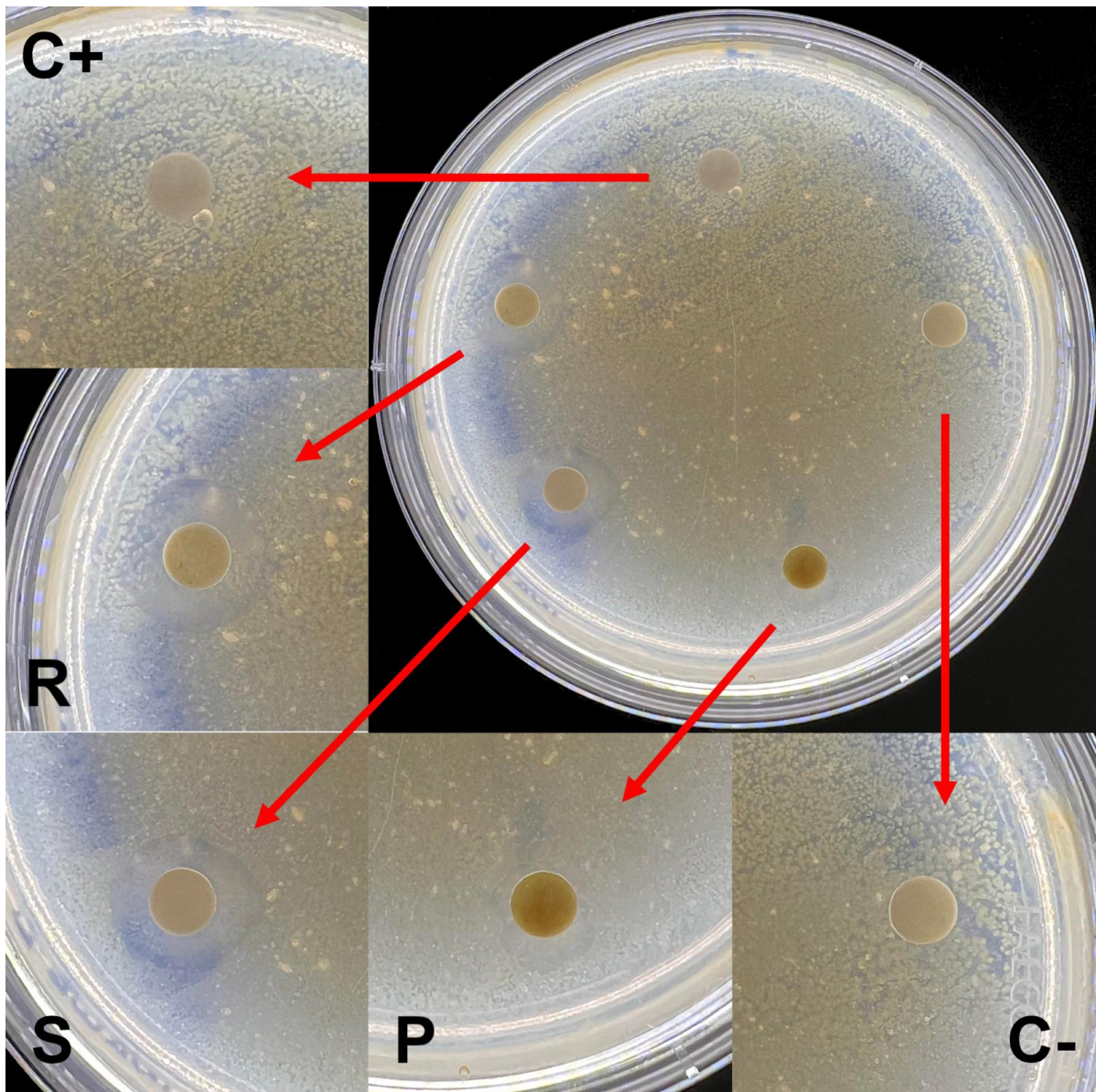
720

721

722 Figure 2: Schematic representation of the inhibition test procedure. The figure outlines the step-  
723 by-step process of assessing potential inhibitory of algal in biofilm as emitter against targeted  
724 algal strains.

725

726



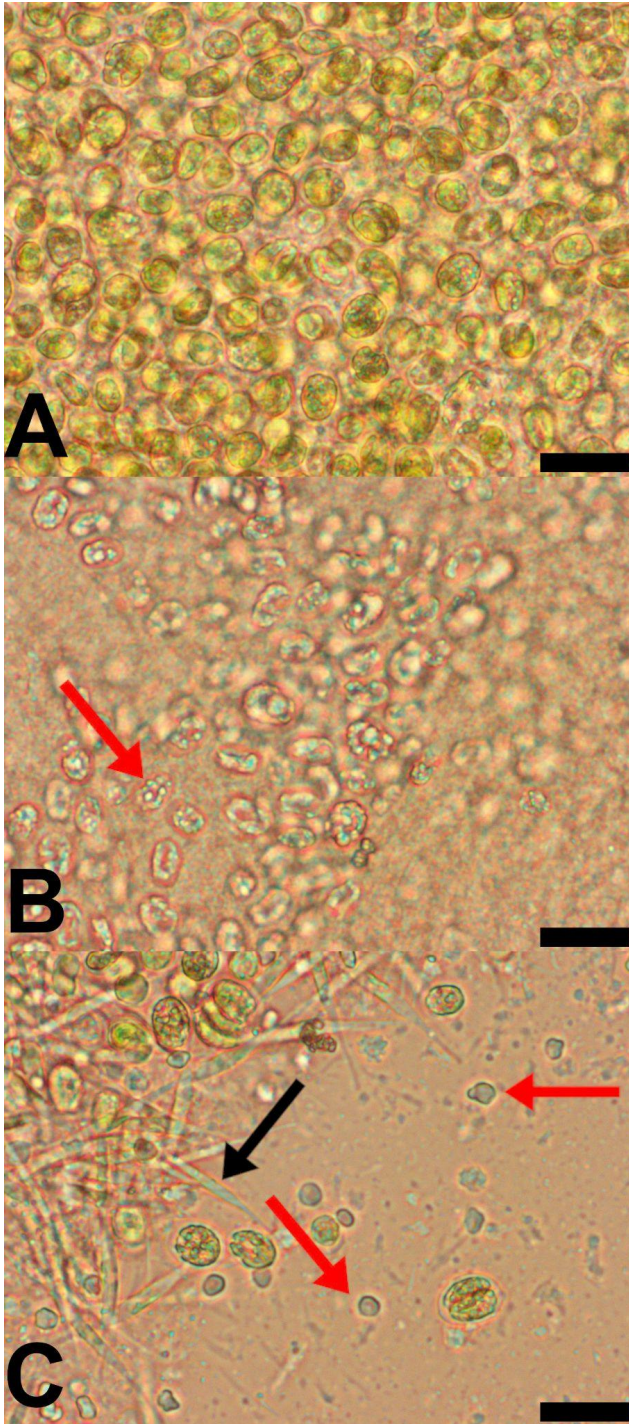
727

728 Figure 3: Example of inhibition assessment using *Nannochloropsis oculata* as target, grown on  
 729 surface agar medium and exposed for 14 days using sterile cellulose disks loaded with test  
 730 samples. C+: positive control (20  $\mu$ L of 35% H<sub>2</sub>O<sub>2</sub>); C-: negative control (20  $\mu$ L sterile f/2  
 731 medium); R: raw paste obtained from the one-week tank bottom biofilm of *Cylindrotheca*  
 732 *closterium* after 14 days of experiment; P: pellet of centrifugated *C. closterium* biofilm; S:  
 733 supernatant of centrifugated *C. closterium* biofilm

734

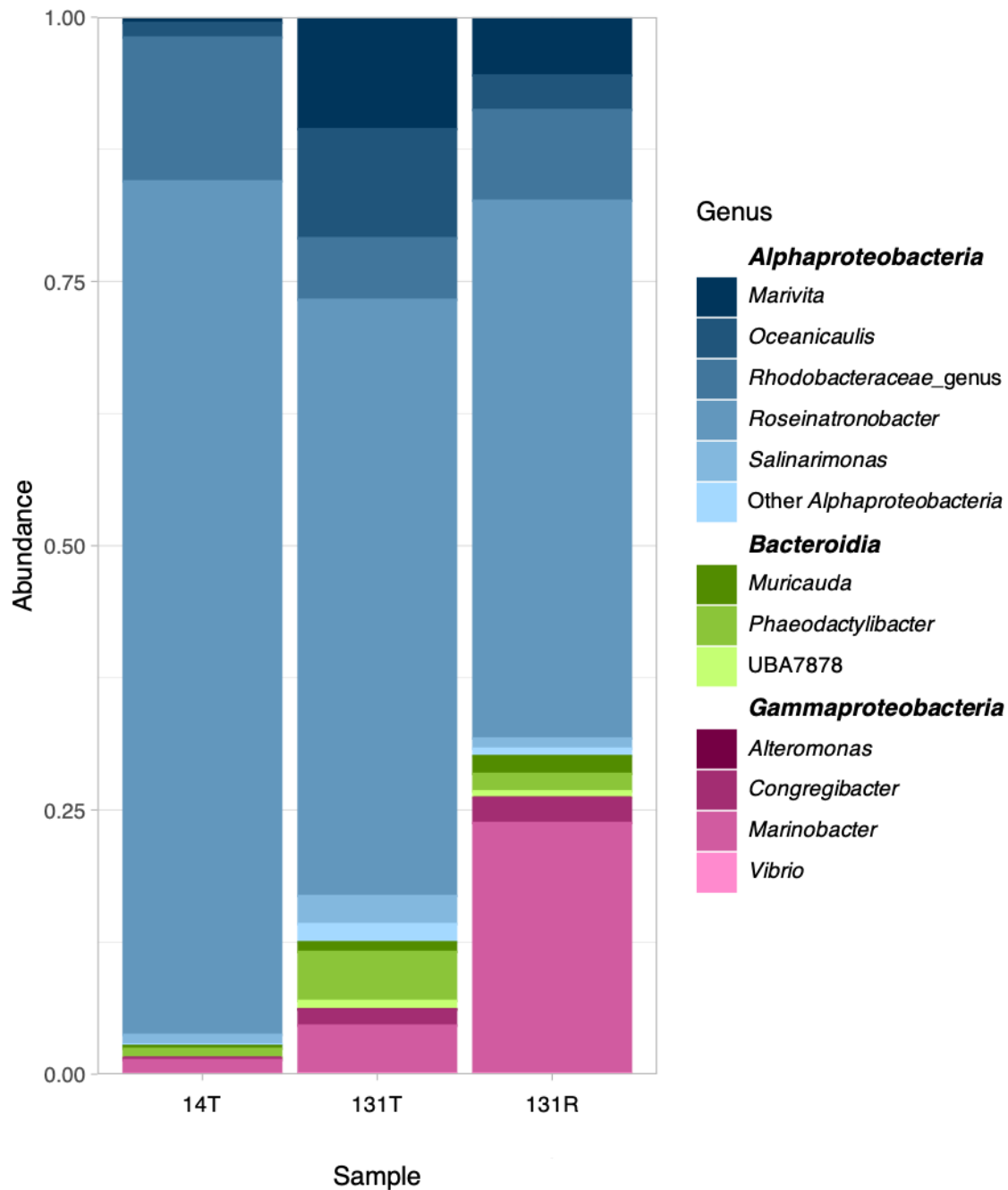
735

736



737

738 Figure 4: Example of exposition to test conditions on *Tetraselmis striata* growing on agar  
 739 medium. A: Culture control. B: Positive control, with the effects of 35% hydrogen peroxide  
 740 (C+ condition) on cell numbers and shape (disrupted cells exemplified by red arrow). C: Sample  
 741 from the inhibition area observed with *C. closterium* biofilm supernatant (S condition) from the  
 742 three-week biofilm from the fabric on the roller after 131 days of experiment, with low  
 743 abundance of *T. striata* including abnormal cells (red arrow) and regrowth of *C. closterium*  
 744 cells (black arrow). Scale bars in black represent 20  $\mu\text{m}$ .



745

746 **Figure 5:** Taxonomic composition of the bacterial community at the genus level, classified at  
 747 the class level, in the 3 samples. Other *Alphaproteobacteria*, *Alphaproteobacteria* genera with  
 748 less sequences than the five most abundant genera in the dataset. (14T: One-week biofilm  
 749 collected from the bottom of the tank after 14 days of experiment (March 24<sup>th</sup> 2023), 131T:  
 750 One-week biofilm collected from the bottom of the tank after 131 days of experiment (July 19<sup>th</sup>  
 751 2023), 131R: Three-week biofilm collected from the fabric of the roller after 131 days of  
 752 experiment (July 24<sup>th</sup> 2023). Details on sequence taxonomic identification are available in  
 753 Supplementary Table 3.